

The MERO Hand: A Mechanically Robust Anthropomorphic Prosthetic Hand using Novel Compliant Rolling Contact Joint*

Huan Liu¹, Kai Xu², Bruno Siciliano¹ and Fanny Ficuciello¹

Abstract—Although substantial progresses have been made in building prosthetic hands, lack of mechanical robustness still restrains wide adoption of robotic hand prostheses. This paper presents the design and evaluation of the MERO hand, which is a MEchanically ROBust anthropomorphic prosthetic hand using novel COmpliant Rolling-contact Element (CORE) joints. The proposed CORE joint, which has a simple structure, exhibits compliance in multiple directions. Its structural parameters were designed, to form underactuated finger designs that can perform adaptive finger motion during grasping. Experiments showed that the hand could withstand severe disarticulation and violent impact. The hand could perform various adaptive grasps and also in-hand manipulation, suggesting that the proposed design might be a viable solution for robust prosthetic hand.

I. INTRODUCTION

Substantial progresses have been made in building anthropomorphic prosthetic hands in the past two decades, using emerging technologies. Currently there are several anthropomorphic hands available in the market, for example the Bebionic Hand (Ottobock GmbH.), the i-Limb Hand (Touch Bionics Ltd.) and the Brunel Hand (Openbionics Ltd.). Research results were also obtained in academia, including the prosthetic hands presented in [1]–[7].

However, prosthetic hands are still under rejection. One of the major reason could be the lack of mechanical robustness [8], [9]. It was reported in [10] that repeated mechanical failure and the high cost of repair and replacement are the major reasons of abandonment of upper-limb prostheses. In particular, workers in labor-intensive or outdoor occupations do not frequently use robotic prostheses, since these hands are susceptible to damage during working [11].

Strong structure and rigid transmission can be adopted to achieve a robust design. For example, the HERI II hand designed for humanoid robot is robust and adaptive to impacts when interacting with the objects and environment [12]. However, bulky rigid parts may increase the weight of a hand, making it not suitable for prosthetic application. Moreover, the approach of increasing rigidity does not coincide with the distinguishing feature of human hand, which is inherently compliant.

*This work was supported by the MUSHA project (Grant agreement No. 320992).

¹Huan Liu (corresponding author), Bruno Siciliano and Fanny Ficuciello are with the Interdepartmental Center for Advances in Robotic Surgery (ICAROS), University of Naples Federico II, 80125 Naples, Italy. E-mail: hzaulihuan@gmail.com, bruno.siciliano@unina.it and fanny.ficuciello@unina.it

²Kai Xu is with the State Key Laboratory of Mechanical System and Vibration, School of Mechanical Engineering, Shanghai Jiao Tong University, Shanghai, China. E-mail: k.xu@sjtu.edu.cn

Inspired by human hand, compliance has been introduced to robotic hands (mainly to the fingers) in different manners, to improve the robustness of prosthetic hands by absorbing external impact.

Compliance can be introduced to the actuation of fingers. The hand of the DLR Hand Arm System [13], with spring mechanism connected to every tendon, allows the fingers to absorb impact. Compliant link made from steel layers, introduced to the hand in [14], enables the fingers to be compliant to lateral forces.

Compliance can be also achieved by finger joints. Flexure joints made from elastic polymer (e.g., polyurethane) were used in the SDM hand [15], the iHY hand [16] and the hand in [1], while a spring-based compliant joint was adopted in the UB Hand 3 design [17]. The PISA/IIT SoftHand [18] and the SoftHand Pro-H [6], using sophisticated COmpliant Rolling-contact Elements (CORE) joint, are particularly interesting to our design.

Soft structure and continuum structure were also attempted, since they allow large deformation under external load. Spring-based continuum finger was used in robotic hand designs in [19], [20], while soft fingers driven by compliant linkage mechanism [14], by pneumatic [21]–[23] and hydraulic power [24] were also proposed. Although robustness was enhanced by soft or continuum mechanisms, concerns may still stem from the increased structural complexity and inadequate grasp force.

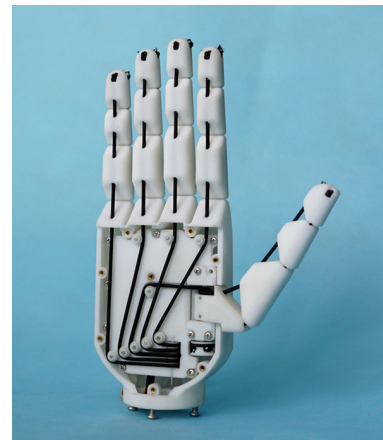


Fig. 1. The developed MERO hand

After evaluating factors such as complexity, weight and cost of different solutions, this paper presents the MERO hand, which is a MEchanically ROBust anthropomorphic prosthetic hand using novel CORE joint, as shown in Fig. 1.

The proposed CORE joint, which has a simple structure fabricated by uncomplicated process, exhibits notable compliance in multiple directions. The kinematics of the joint was modeled and verified.

The fingers of the MERO hand can resist various disarticulation (e.g., backward bend, sideway bend, twist and dislocation), benefiting from serially connected CORE joints.

Experiments verified that the hand can perform various grasps and also in-hand manipulation. Tests were conducted to show that the hand can tolerate severe disarticulation and violent impact, demonstrating the robustness of the design.

This paper is organized as follows. In Section II, introduction and modeling of the novel CORE joint are presented. Section III describes the design details of the MERO hand. Experimental characterizations are reported in Section IV with the conclusions and future directions summarized in Section V.

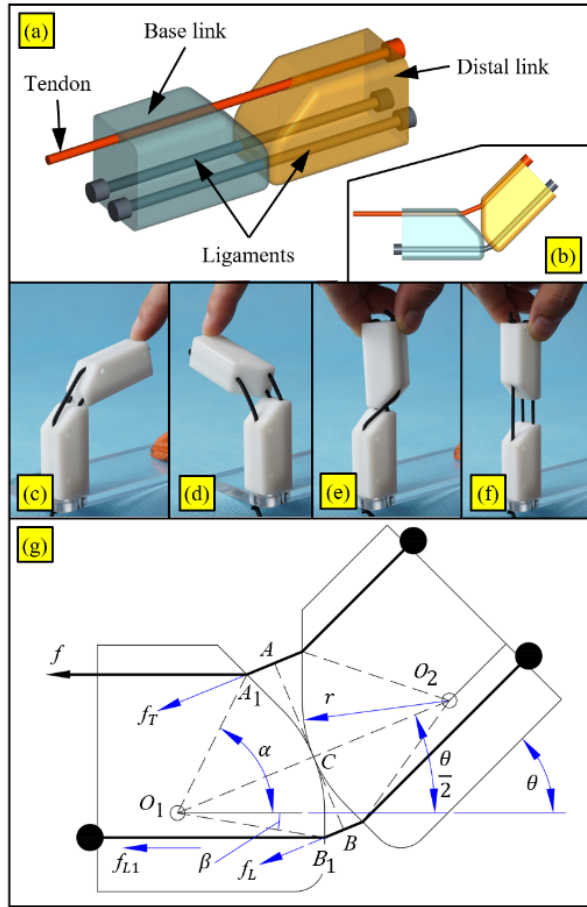


Fig. 2. The proposed CORE joint: (a) extended configuration, (b) bent configuration, (c) backward bend, (d) sideway bend, (e) twist, (f) dislocation, and (g) modeling of the joint

II. THE COMPLIANT ROLLING CONTACT JOINT

Compliant Rolling-contact Elements (CORE) [25] consists of a pair of surfaces in rolling contact with each other, with elastic elements holding them together. Several CORE joints were proposed, including the joints patented in [26],

[27] and the CORE joint used in the PISA/IIT SoftHand [18] and the SoftHand Pro-H [6].

This paper proposes a novel CORE joint, as shown in Fig. 2, which achieves multi-directional compliance using a straightforward structure. The joint consists of a base link, a distal link, two ligaments and a tendon, as shown in Fig. 2(a). The ligaments, made of elastic strings, are attached to the base link and the distal link. The tendon, which is also elastic, is anchored to the distal link and threaded through the hole of the base link. At the extended configuration shown in Fig. 2(a), two facets of the links were held together by the elastic ligaments.

By pulling the tendon, the distal link is actuated and rolled on the cylindrical surface of the base link, as shown in Fig. 2(b). Once the tendon is released, the elastic ligaments return the distal link to the extended position, similar to a torsional spring in a conventional pin joint. The elastic tendon and ligaments bring the joint multi-directional compliance, by allowing various disarticulation, including backward bend, sideway bend, twist and dislocation, as shown in Fig. 2(b) – (f), respectively.

The CORE joints in [27] use several intersected flexible metal bands or ribbons as elastic elements. Due to high elastic modulus of the metal bands or ribbons, the joint might be too stiff to allow large undesired deformation. The PISA/IIT SoftHand [18] and the SoftHand Pro-H [6] use elastic strings to hold phalanges together, which tolerate larger deformation of the finger joints.

The structure of the proposed CORE joint was largely simplified and unnecessary features were removed, compare to the CORE joints of the PISA/IIT SoftHand and the SoftHand Pro-H. For example, the CORE joint of the Pisa/IIT hand has a mechanical limit that stops the joint at the extended position, while the CORE joint in this research has two facets held together by the ligaments that ensures extend configuration of the joint.

In this research, the tendons and ligaments were made from low-cost elastic string, which is originally for clothing industry. It composed of rubber strands forming a core, wrapped in polypropylene braided covering. The stiffness of the string was observed highly non-linear from experiments. Therefore, we assume the tension t of a stretched string segment is give by a non-linear function as:

$$t = T(l_0, \Delta l) \quad (1)$$

where l_0 and Δl is the free length and the elongation of the string segment, respectively.

The modeling of the joint is illustrated in Fig. 2(g). As an actuation force f is pulling the tendon, the distal link rotates an angle θ .

The tension on the tendon and the ligaments between the two links is denoted by f_T and f_L , respectively. They are subject to:

$$f_T \|CA\| = f_L \|CB\| \quad (2)$$

Force arms $\|CA\|$ and $\|CB\|$ in (2) can be calculated by:

$$\|CA\| = \|O_1 A_1\| \sin(\alpha - \frac{\theta}{2}) \quad (3)$$

$$\|CB\| = \|O_1B_1\| \sin(\beta + \frac{\theta}{2}) \quad (4)$$

where $\|O_1A_1\|$, α and $\|O_1B_1\|$, β gives the positions at which the tendon and the ligament thread out of the base link, respectively.

Because of friction, f and f_T are related as:

$$f = f_T \cos(\frac{\theta}{2}) + \mu f_T \sin(\frac{\theta}{2}) \quad (5)$$

where μ is the friction coefficient between the string and the rigid link. Here the friction is assumed centralized at the point where the string thread out of the link.

Similarly, f_{L1} , which is the tension on the ligament segment inside the base link, is related to f_L by:

$$f_L \cos(\frac{\theta}{2}) = f_{L1} + \mu f_L \sin(\frac{\theta}{2}) \quad (6)$$

The tension f_{L1} can be calculated by:

$$f_{L1} = 2T(\frac{l_0}{2}, \|B_1B\| + \frac{l_p}{2}) \quad (7)$$

where l_0 and l_p is the free length and the preload of the ligament, respectively. $\|B_1B\|$ is the length increment of the ligament compare to the extended configuration of the joint, which is given by:

$$\|B_1B\| = r - \|O_1B_1\| \cos(\beta + \frac{\theta}{2}) \quad (8)$$

where r is the radius of the cylindrical surface.

Therefore, given a actuation force f , joint angle θ can be solved by (1) – (8). Or vice versa, given a joint angle θ , actuation force f can be calculated use the same equations.

III. DESIGN DESCRIPTIONS OF THE MERO HAND

The MERO hand has an anthropomorphic appearance in a size of human hand, as shown in Fig. 1 and Fig. 3(a). The length of the hand (from the tip of the middle finger to the wrist) is 220mm, while the width of the palm is 80mm. The total weight of the hand is 336g, without control electronics and power supply.

This section presents design descriptions of the MERO hand. The actuation strategy is summarized in Section III.A and the finger design based on the CORE joint is presented in Section III.B.

A. Actuation Strategy

The MERO hand has 16 joints in total. Each finger has three flexion/extension joints made from the proposed CORE joint, while the thumb has one additional pin joint for thumb rotation. Letters T and I before the underscore indicate the joints for the thumb and the index finger respectively, as shown in Fig. 3. Abbreviations of rot, abd, mcp, ip, pip and dip indicate the rotation joint, the abduction joint, the metacarpophalangeal joint, the interphalangeal joint, the proximal and the distal interphalangeal joint respectively.

Three CORE joints of each finger (e.g., T_abd, T_mcp and T_ip joint of the thumb) are driven by one elastic tendon, to form a underactuated design.

The idea is of using coordinated motions inspired by the human hand for robotic applications that is demonstrated to be the keystone towards smart hands simple to build and control while retaining much of the human hand functionality and skills [28]. In general, the use of synergies creates a valid alternative that overcomes the limits of model-based methods for control and full-actuation trends for design [29]–[31].

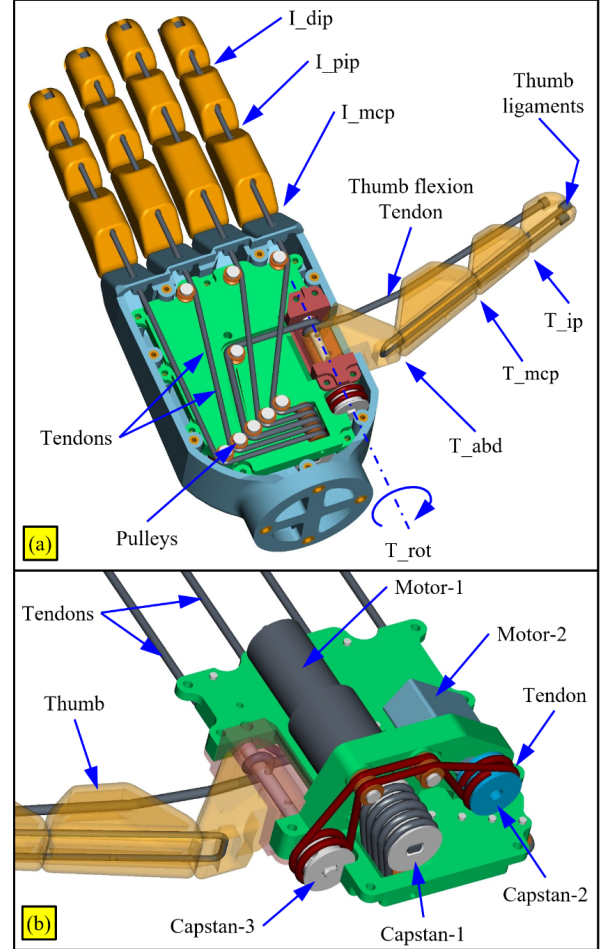


Fig. 3. Design of the MERO hand: (a) finger joints and (b) actuation

The flexion of all fingers were decided to be driven by one motor, as evidence showed strong coupling between flexion of all fingers [32]. Since the driving tendons are elastic, the fingers can adapt to grasped object therefore adaptive hand configuration can be formed.

Underactuation based on compliant transmission have been used in robotic hand designs, for example in the TBM hand [33] and the Michelangelo Hand (Ottobock GmbH.). The MERO hand adopted a simpler design, as shown in Fig. 3(b). The finger flexion tendons start from fingertips and thread through joints and pulleys, then wind on the Capstan-1 mounted on the Motor-1 (Maxon DCX16s 4.5W with 101.2:1 gearbox). Therefore, no additional mechanism (e.g., pulleys or linkages in differential mechanisms) is needed. The MERO hand is expected to have better robustness, benefiting from its structural simplicity.

The rotation of the thumb is designed to be independently driven by the second motor. Studies on fully actuated robotic hands demonstrate that thumb adduction/abduction motion depends especially from the third synergy that is responsible of successful precision grasps [34]–[37]. Considering the important role of the thumb on grasp stability, in particular for the opposition role, we decided to use the second motor for adduction/abduction thumb motion. This motor can rotate the thumb during the grasp by creating synergies with the closure movement, thus providing internal manipulation capabilities. Although single-actuator hands (e.g. the Pisa/IIT hand [18] and the SoftHand Pro-H hand [6]) could perform various grasps, independent rotation of the thumb can further enhance grasp versatility. For example, the MERO hand could grasp a credit card using the thumb and the lateral of the index finger, which is usually refer to as lateral grasp.

Some robotic hands adopted passive thumb rotation design. For example, the thumb of the commercial Bebionic V3 Hand and the hand in [3] can be manually configured to different positions. However, a motorized rotation joint offers the possibility of in-hand manipulation. Fig. 4 shows a example of manipulating a cylinder using three fingers. The hand grasps a cylinder by tripod pinch. By only driving the thumb rotation joint, the cylinder can be rotated.

During this manipulation, the contact of the fingers and the object is maintained by the elastic strings and no special control strategy or tactile/position feedback is required. The compliant transmission alleviates the need of complicated mechanronic design and coordinated control of multiple finger joints. Furthermore, the Motor-2 (ES08A II Servo Motor from Yinyan, Co. Ltd., China) costs less than three Euros. It weighs only 12g, which is only 3.6% of the total weight of the MERO hand.

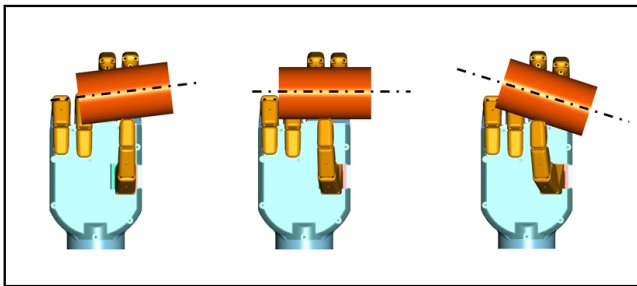


Fig. 4. The schematic of the MERO hand manipulating a cup

As shown in Fig. 3, the tendon for the thumb flexion is routed around the thumb rotation shaft, while the T_rot joint is independently driven by the Motor-2. The same elastic string was used to couple the Capstan-2 and the Capstan-3, which is mounted on the Motor-2 and the thumb, respectively. Therefore, the T_rot joint is also compliant, due to the elastic transmission.

The control and actuation hardware using commercially available electronic components was designed as shown in Fig. 5. An Arduino UNO as a controller receives control commands from a PC via its serial port. It controls the Motor-

1 via a L298N motor driver and controls the Motor-2 directly.

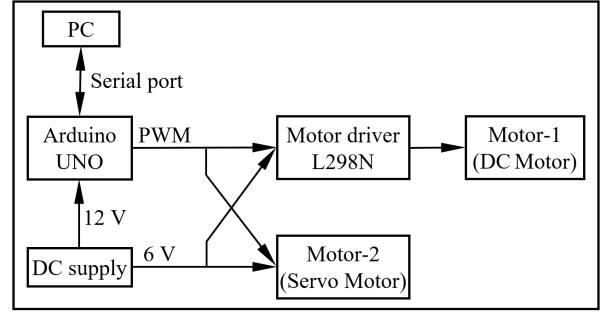


Fig. 5. Schematic of the control and actuation hardware

B. Finger Design based on the CORE Joint

The MERO hand has five fingers with similar finger design, as each finger has three serially connected CORE joints driven by one elastic tendon.

Take the index finger as an example, the I_mcp, I_pip and I_dip joints are driven by one elastic tendon, as shown in Fig. 6(a). When the driving tendon is pulled, the three joints flex at the same time.

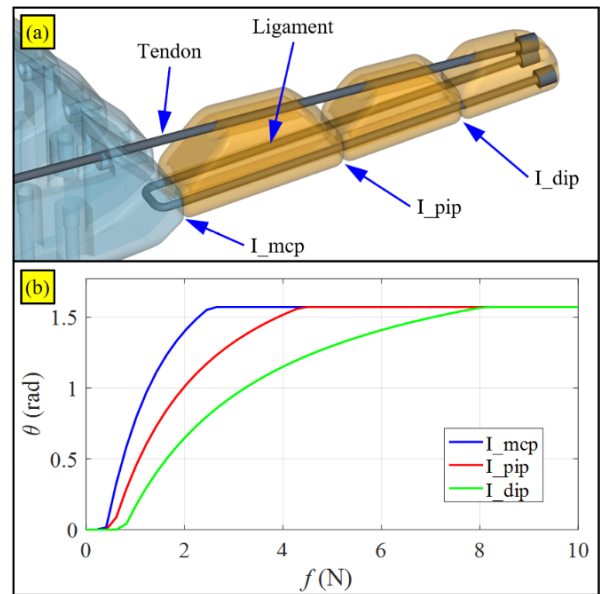


Fig. 6. The index finger based on the CORE joints: (a) schematic and (b) simulated joint angles

It is preferable that the I_mcp joint rotates faster than the I_pip and the I_dip joint, therefore the proximal phalange will encounters an object first during power grasp. Then continuing to pull the tendon will close the I_pip and I_dip joints, thus conforming finger configuration can be formed.

The parameters listed in Table I were chosen, considering the constraints from anthropomorphic appearance. Using the modeling presented in Section II, the angle of each finger joint was calculated and plotted in Fig. 6. Elastic string with a diameter of $\phi 2$ mm was chosen for the CORE joint. The

TABLE I
STRUCTURAL PARAMETERS OF THE FINGER JOINTS

$\beta = 0.38$ rad		$\ OB_1\ = 5.4$ mm	
$r = 5$ mm			
Thumb			
	abd	mcp	ip
α	1.94 rad	1.89 rad	1.63 rad
$\ OA_1\ $	17.1 mm	10.1 mm	7.5 mm
Fingers (except the thumb)			
	mcp	pip	dip
α	1.93 rad	1.74 rad	1.4 rad
$\ OA_1\ $	12.3 mm	8.6 mm	6.1 mm
Tendon stiffness			
$T(l_0, \Delta l) = 9.6(\frac{\Delta l}{l_0})^4 + 6.4(\frac{\Delta l}{l_0})^3 - 20(\frac{\Delta l}{l_0})^2 + 11.26\frac{\Delta l}{l_0} + 0.39$			

tension of the string under different elongation was measured then a fourth-order polynomial regression of the measured results was adopted, as listed in Table I.

As indicated by the figure, the L_{mcp} joint flexes faster than the L_{pip} and the L_{dip} joint and it reaches its joint limit ($\pi/2$) earlier than the L_{pip} and L_{dip} joint. This feature ensures the fingers adaptively wrap around an object in power grasp.

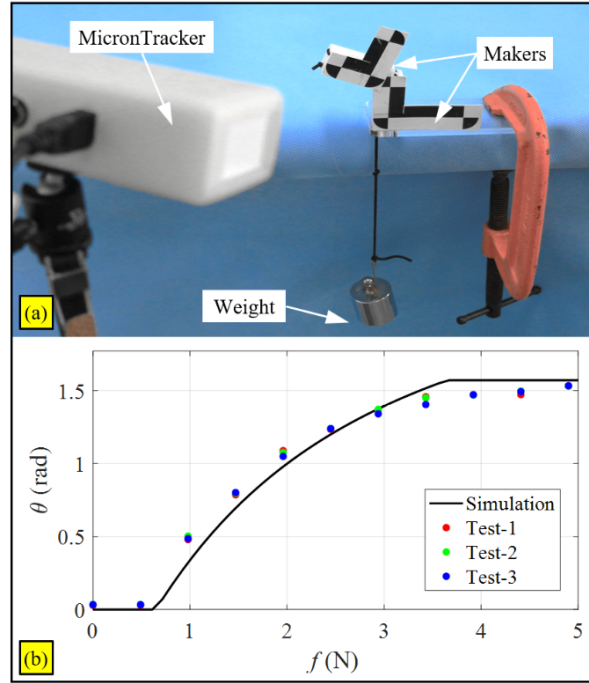


Fig. 7. Characterization of the CORE joint: (b) experimental setup, (c) simulated and measured results of the joint kinematics

IV. EXPERIMENTAL CHARACTERIZATIONS

In order to evaluate the effectiveness of the proposed CORE joints and the MERO hand, three sets of experiments were conducted. A video is included to show the experimentation of the compliant joint and the MERO hand.

A. Characterization of the CORE Joint

A CORE joint was designed using the structure parameters listed in Table II.

TABLE II
STRUCTURE PARAMETERS OF A SINGLE CORE JOINT

$\alpha = 1.85$ rad	$\ OA_1\ = 10.4$ mm	$l_0 = 70$ mm	$\mu = 0.25$
$\beta = 0.38$ rad	$\ OB_1\ = 5.4$ mm	$l_p = 15$ mm	$r = 5$ mm

The joint kinematics was characterized, using the experimental setup shown in Fig. 7(a). Two markers were attached to the base link and the distal link. An optical tracker (MicronTracker SX60, Claron Technology Inc.) was used to measure the positions and orientations of the markers. Then the orientation of the distal link with respect to the base link can be calculated. The weight hanging on the tendon was increased with 50g increment until the joint reached its limit ($\pi/2$). The measurement was repeated for three times.

The measured results were plotted in Fig. 7(b), together with the simulated results calculated by the modeling presented in Section II. It can be seen from Fig. 7(b) that the measured results well matched the modeling. The CORE joint has a good repeatability, as the standard deviation between the three sets of the measured results is lower than 1.8° .

B. Grasp and Manipulation Experiments

1) *Grasp*: To evaluate its grasping capability, the hand was commanded to grasp various objects. The hand could perform grasp patterns including power grasp, pinch and lateral grasp, as shown in Fig. 8(a), (b) and (c), respectively.

The motor was always powered on at 6.0V till the grasp is completed and the motor is stalled. A clutch might be needed in a future design to avoid overheating the motor as well as reduce power consumption.

The fingers adapted to different shapes of the objects, due to the underactuated finger design and the elastic tendon transmission.

Take the power grasps shown in Fig. 8(a) as examples, once the proximal phalanges were stopped by the object, continuing to pull the tendons closes the pip and then the dip joints, thus conforming finger configuration is formed.

The contribution of the elastic tendon transmission is mostly notable in the left-most photo of Fig 8(b), as the hand is pinching a foam plate, which was intentionally cut to the irregular shape. As the index and the middle finger were stopped by the plate, the ring and the little finger continued to flex until the adaptive grasp formed.

The grasping force of the hand was also quantified, as shown in the right-most photo of Fig. 8(a). A 3D-printed cylinder of 60 mm diameter, with a force sensor (ATI Nano 17) installed inside, was held by the hand using power grasp. The hand motor was powered at 6.0V to stall the motor. The quantification was repeated for three times. The average grasp force is 3.6N. It is worth noting that, the sparse arrangement of the components inside in the palm leaves us a possibility to boost up the grasp force by adopting more powerful motor.

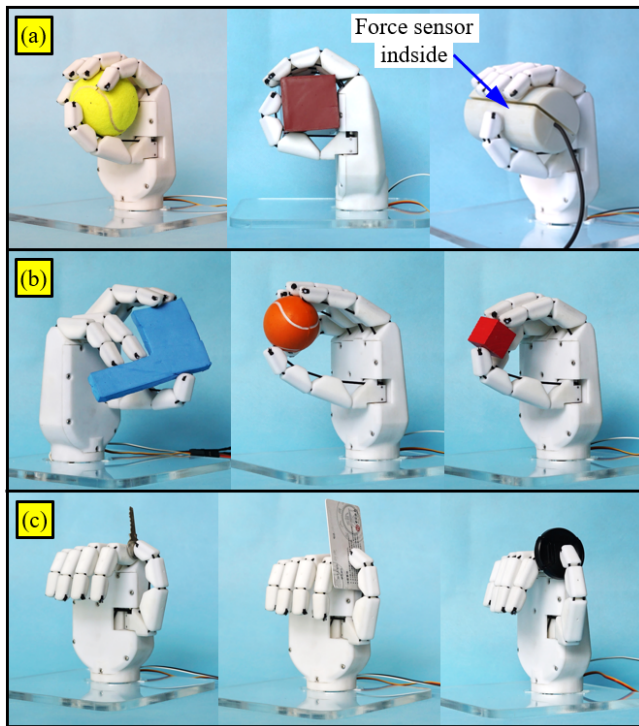


Fig. 8. Grasping experiments: (a) power grasps, (b) pinches and (c) lateral grasps experiments

2) *Manipulation*: In-hand manipulation capability was also tested. The MERO hand was commanded to perform in-hand manipulation as shown in Fig. 9. The $\phi 50\text{mm}$ plastic cup was pinched, using the fingertips of the thumb, the middle and the index finger. Then the Motor-2 drove the rotation joint of the thumb from 85° to 110° . The cup was rotated 16.8° (from the left to the right photo).

During this manipulation, only the Motor-2 was driven. The Motor-1 was switched off and the hand maintained contact with the object due to the elastic strings. Usually finger joints of a fully-actuated hand need to be coordinately controlled to maintain constant contact with an object, during in-hand manipulation. However, the compliant transmission of the MERO hand alleviated the demand of complicated control.

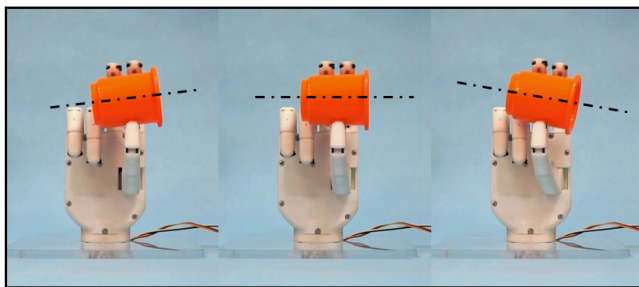


Fig. 9. The MERO hand rotating a cup by its fingertips (from left to right)

C. Test of Robustness

To verify the mechanical robustness of the MERO hand, three sets of experiments were conducted. These tests are designed to mimic the situation that the hand is bumped to surroundings by accident, when it is used as a prosthetic hand.

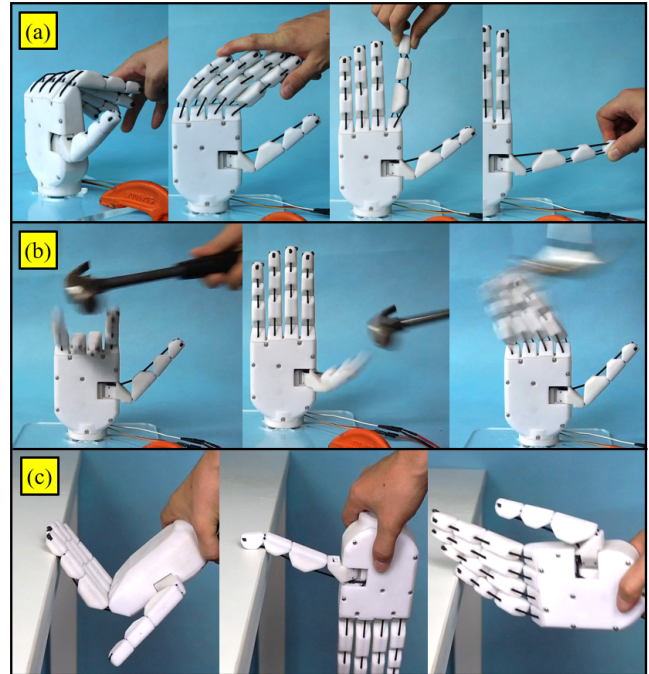


Fig. 10. Tests of robustness: (a) the fingers under disarticulation, (b) the hand during impacts with a hammer and (c) a table

First, the fingers were intentionally disarticulated, including backward bend, sideways bend, twist and dislocation, as shown in Fig. 10(a). The phalanges restored their correct positions, after the removal of external force. The tests caused no damage to the joints or the elastic strings.

Then the capability to withstand violent impacts was tested. The hand was rigidly mounted to a table and then hit by a hammer, as shown in Fig. 10(b). After that, the hand was bumped on a table by its fingers, as shown in Fig. 10(c). The fingers also restored their correct configurations without any damage, after swinging back and forth for few times.

As demonstrated by above tests, the fingers of the MERO hand could withstand various deformation, due to the compliant joint design. This feature would be valuable when the hand is used in interaction with unstructured environment, for example being used as a prosthetic hand.

V. CONCLUSIONS AND FUTURE WORK

To improve the mechanical robustness of prosthetic hand, this paper presents the design, construction and experimentation of an anthropomorphic hand using novel compliant joint. The proposed CORE joint has a simple structure made by uncomplicated process, exhibits multi-axial compliance.

The MERO hand could perform various grasps and also in-hand manipulation. The hand exhibited notable robustness in experiments, suggesting it could be a viable solution for robust anthropomorphic prosthetic hand.

Future efforts will first be directed to increase the grasp force for practical prosthetic application. Structural parameters of finger design based on the CORE joint will also be deeply investigated and optimized, toward better grasp performance and also larger manipulation workspace.

REFERENCES

- [1] J. T. Belter and A. M. Dollar, "Novel differential mechanism enabling two dof from a single actuator: Application to a prosthetic hand," in *Rehabilitation Robotics (ICORR), 2013 IEEE International Conference on*, pp. 1–6, IEEE, 2013.
- [2] K. Xu, H. Liu, Y. Du, and X. Zhu, "Design of an underactuated anthropomorphic hand with mechanically implemented postural synergies," *Advanced Robotics*, vol. 28, no. 21, pp. 1459–1474, 2014.
- [3] K. Xu, H. Liu, Z. Liu, Y. Du, and X. Zhu, "A single-actuator prosthetic hand using a continuum differential mechanism," in *Robotics and Automation (ICRA), 2015 IEEE International Conference on*, pp. 6457–6462, IEEE, 2015.
- [4] T. Lenzi, J. Lipsey, and J. W. Sensinger, "The ric armla small anthropomorphic transhumeral prosthesis," *IEEE/ASME Transactions on Mechatronics*, vol. 21, no. 6, pp. 2660–2671, 2016.
- [5] M. Controzzi, F. Clemente, D. Barone, A. Ghionzoli, and C. Cipriani, "The ssa-myhand: a dexterous lightweight myoelectric hand prosthesis," *IEEE Transactions on Neural Systems and Rehabilitation Engineering*, vol. 25, no. 5, pp. 459–468, 2017.
- [6] C. Piazza, M. G. Catalano, S. B. Godfrey, M. Rossi, G. Grioli, M. Bianchi, K. Zhao, and A. Bicchi, "The soft-hand pro-h: a hybrid body-controlled, electrically powered hand prosthesis for daily living and working," *IEEE Robotics & Automation Magazine*, vol. 24, no. 4, pp. 87–101, 2017.
- [7] K. Xu, H. Liu, Z. Zhang, and X. Zhu, "Wrist-powered partial hand prosthesis using a continuum whiffle tree mechanism: A case study," *IEEE Transactions on Neural Systems and Rehabilitation Engineering*, vol. 26, no. 3, pp. 609–618, 2018.
- [8] E. A. Biddiss and T. T. Chau, "Upper limb prosthesis use and abandonment: a survey of the last 25 years," *Prosthetics and orthotics international*, vol. 31, no. 3, pp. 236–257, 2007.
- [9] K. Østlie, I. M. Lesjø, R. J. Franklin, B. Garfelt, O. H. Skjeldal, and P. Magnus, "Prosthesis rejection in acquired major upper-limb amputees: a population-based survey," *Disability and Rehabilitation: Assistive Technology*, vol. 7, no. 4, pp. 294–303, 2012.
- [10] K. Bhaskaranand, A. K. Bhat, and K. N. Acharya, "Prosthetic rehabilitation in traumatic upper limb amputees (an indian perspective)," *Archives of orthopaedic and trauma surgery*, vol. 123, no. 7, pp. 363–366, 2003.
- [11] F. Cordella, A. L. Ciancio, R. Sacchetti, A. Davalli, A. G. Cutti, E. Guglielmelli, and L. Zollo, "Literature review on needs of upper limb prosthesis users," *Frontiers in neuroscience*, vol. 10, p. 209, 2016.
- [12] Z. Ren, N. Kashiri, C. Zhou, and N. G. Tsagarakis, "Heri ii: A robust and flexible robotic hand based on modular finger design and under actuation principles," in *2018 IEEE/RSJ International Conference on Intelligent Robots and Systems (IROS)*, pp. 1449–1455, Oct 2018.
- [13] M. Grebenstein, M. Chalon, W. Friedl, S. Haddadin, T. Wimböck, G. Hirzinger, and R. Siegwart, "The hand of the dlr hand arm system: Designed for interaction," *International Journal of Robotics Research*, vol. 31, no. 13, pp. 1531–1555, 2012.
- [14] K. Y. Choi, A. Akhtar, and T. Bretl, "A compliant four-bar linkage mechanism that makes the fingers of a prosthetic hand more impact resistant," in *Robotics and Automation (ICRA), 2017 IEEE International Conference on*, pp. 6694–6699, IEEE, 2017.
- [15] A. M. Dollar and R. D. Howe, "The highly adaptive sdm hand: Design and performance evaluation," *The international journal of robotics research*, vol. 29, no. 5, pp. 585–597, 2010.
- [16] L. U. Odhner, L. P. Jentoft, M. R. Claffee, N. Corson, Y. Tenzer, R. R. Ma, M. Buehler, R. Kohout, R. D. Howe, and A. M. Dollar, "A compliant, underactuated hand for robust manipulation," *The International Journal of Robotics Research*, vol. 33, no. 5, pp. 736–752, 2014.
- [17] F. Lotti, P. Tiezzi, G. Vassura, L. Biagiotti, G. Palli, and C. Melchiorri, "Development of ub hand 3: Early results," in *ICRA*, pp. 4488–4493, 2005.
- [18] M. G. Catalano, G. Grioli, E. Farnioli, A. Serio, C. Piazza, and A. Bicchi, "Adaptive synergies for the design and control of the pisa/fit soft-hand," *The International Journal of Robotics Research*, vol. 33, no. 5, pp. 768–782, 2014.
- [19] J. Potratz, J. Yang, K. Abdel-Malek, E. P. Pitarch, and N. Grosland, "A light weight compliant hand mechanism with high degrees of freedom," *Journal of biomechanical engineering*, vol. 127, no. 6, pp. 934–945, 2005.
- [20] S. Makino, K. Kawaharazuka, M. Kawamura, Y. Asano, K. Okada, and M. Inaba, "High-power, flexible, robust hand: Development of musculoskeletal hand using machined springs and realization of self-weight supporting motion with humanoid," in *Intelligent Robots and Systems (IROS), 2017 IEEE/RSJ International Conference on*, pp. 1187–1192, IEEE, 2017.
- [21] M. A. Devi, G. Udupa, and P. Sreedharan, "A novel underactuated multi-fingered soft robotic hand for prosthetic application," *Robotics and Autonomous Systems*, vol. 100, pp. 267–277, 2018.
- [22] H. Zhao, K. O'Brien, S. Li, and R. F. Shepherd, "Optoelectronically innervated soft prosthetic hand via stretchable optical waveguides," *Science Robotics*, vol. 1, no. 1, p. eaai7529, 2016.
- [23] J. Zhou, J. Yi, X. Chen, Z. Liu, and Z. Wang, "Bcl-13: A 13-dof soft robotic hand for dexterous grasping and in-hand manipulation," *IEEE Robotics and Automation Letters*, vol. 3, no. 4, pp. 3379–3386, 2018.
- [24] S. Schulz, C. Pylatiuk, M. Reischl, J. Martin, R. Mikut, and G. Bretthauer, "A hydraulically driven multifunctional prosthetic hand," *Robotica*, vol. 23, no. 3, pp. 293–299, 2005.
- [25] J. R. Cannon, C. P. Lusk, and L. L. Howell, "Compliant rolling-contact element mechanisms," in *ASME 2005 International Design Engineering Technical Conferences and Computers and Information in Engineering Conference*, pp. 3–13, American Society of Mechanical Engineers, 2005.
- [26] B. M. Hillberry and A. S. Hall Jr, "Rolling contact joint," Jan. 13 1976. US Patent 3,932,045.
- [27] C. F. Ruoff, "Rolling contact robot joint," Dec. 17 1985. US Patent 4,558,911.
- [28] C. D. Santana, G. Grioli, M. Catalano, A. Brando, and A. Bicchi, "Dexterity augmentation on a synergistic hand: The Pisa/IIT Soft-Hand+," in *Proc IEEE-RAS 15th Int Conf on Humanoid Robots*, (Seoul, Korea), pp. 497–503, 2015.
- [29] F. Ficuciello, R. Carloni, L. Visser, and S. Stramigioli, "Port-hamiltonian modeling for soft-finger manipulation," in *Proc IEEE/RSJ Int Conf on Intelligent Robots and Systems*, (Taipei, Taiwan), p. 4281–4286, 2010.
- [30] F. Ficuciello, G. Palli, C. Melchiorri, and B. Siciliano, "Planning and control during reach to grasp using the three predominant UB Hand IV postural synergies," in *Proc IEEE Int Conf on Robotics and Automation*, (Saint Paul), pp. 2255–2260, 2012.
- [31] F. Ficuciello, D. Zaccara, and B. Siciliano, "Synergy-based policy improvement with path integrals for anthropomorphic hands," in *Proc IEEE Int Conf on Intelligent Robots and Systems*, (Daejeon, Korea), pp. 1940–1945, 2016.
- [32] M. Santello, M. Flanders, and J. F. Soechting, "Postural hand synergies for tool use," *Journal of Neuroscience*, vol. 18, no. 23, pp. 10105–10115, 1998.
- [33] N. Dechev, W. Cleghorn, and S. Naumann, "Multiple finger, passive adaptive grasp prosthetic hand," *Mechanism and machine theory*, vol. 36, no. 10, pp. 1157–1173, 2001.
- [34] M. Gabiccini and A. Bicchi, "On the role of hand synergies in the optimal choice of grasping forces," in *Proc. of Robotics: Science and Systems*, (Zaragoza), 2010.
- [35] F. Ficuciello, G. Palli, C. Melchiorri, and B. Siciliano, "A model-based strategy for mapping human grasps to robotic hands using synergies," in *Proc IEEE/ASME International Conference on Advanced Intelligent Mechatronics (AIM)*, (Wollongong, Australia), pp. 1737–1742, 2013.
- [36] F. Ficuciello, G. Palli, C. Melchiorri, and B. Siciliano, *Postural Synergies and Neural Network for Autonomous Grasping: a Tool for Dexterous Prosthetic and Robotic Hands*, ch. Converging Clinical and Engineering Research on Neurorehabilitation, Biosystems and Biorobotics, pp. 467–480. Springer Berlin Heidelberg, 2012.
- [37] F. Ficuciello, "Synergy-based control of underactuated anthropomorphic hands," *IEEE Transactions on Industrial Informatics*, vol. 15, pp. 1144–1152, Feb 2019.